

QSO Lensing Magnification: A Comparison of 2QZ and SDSS Results

G. Mountrichas* & T. Shanks

Department of Physics, University of Durham, South Road, Durham DH1 3LE, UK

21 March 2006

ABSTRACT

The lensing magnification of background QSOs by foreground galaxies and clusters is a powerful probe of the mass density of the Universe and the power spectrum of mass clustering. However, the observational results in this area have been controversial. In particular, the 2dF QSO survey suggests that a strong anticorrelation effect at $g < 21$ is seen for both galaxies and clusters which implied that galaxies are anti-biased ($b \approx 0.1$) on small scales at a higher level than predicted by the standard cosmology (Myers et al., 2003, 2005) whereas results from SDSS suggested that the effect was much smaller ($b \approx 1$) and in line with standard expectations (Scranton et al., 2005).

We first cross-correlate the SDSS photo- z , $g < 21$, $1.0 < z_p < 2.2$ QSOs with $g < 21$ galaxies and clusters in the same areas. The anti-correlation found is somewhat less than the results of Myers et al. based on 2QZ QSOs. But contamination of the QSOs by low redshift NELGs and QSOs can cause underestimation of the anticorrelation lensing signal. Correcting for such low redshift contamination at the levels indicated by our spectroscopic checks suggests that the effect is generally small for QSO cross-correlations with $g < 21$ galaxies but may be an issue for fainter galaxy samples. Thus when this correction is applied to the photo- z QSO sample of Scranton et al. the anti-correlation increases and the agreement with the 2QZ results of Myers et al. is improved. When we also take into account the fainter $r < 21$ galaxy limit of Scranton et al. as opposed to $g < 21$ for Myers et al., the two observational results appear to be in very good agreement. This therefore leaves open the question of why the theoretical interpretations are so different for these analyses. We note that the results of Guimaraes, Myers & Shanks based on mock catalogues from the Λ CDM Hubble Volume strongly suggest that QSO lensing at the levels detected by both Myers et al. and now Scranton et al. is incompatible with a galaxy bias of $b \approx 1$ in the standard cosmological model. If the QSO lensing results are correct then the consequences for cosmology may be significant (see Shanks 2006).

Key words: gravitational lensing

1 INTRODUCTION

Large concentrations of mass at low redshift such as galaxies and groups of galaxies can gravitationally lens background objects such as galaxies, QSOs, supernovae and the cosmic microwave background. This phenomenon affects these background sources in two ways. It magnifies and distorts them. This systematic distortion is called cosmic shear (see e.g. Mellier and Meylan 2005 for a review) and the magnification cosmic magnification (Wu 1994, Broadhurst et al. 1995). In turn cosmic magnification has also two effects named the solid angle and amplification effect. The amplifi-

cation effect brightens the apparent magnitude of the background sources resulting in an increase of the objects that we observe in a magnitude limited survey whereas for the solid angle effect, the lensing effectively reduces the solid angle behind the lens, decreasing the number of background sources. These two competing effects are responsible for the different results expected for different magnitude QSO samples. So for bright QSO samples with a steep number count slope the amplification effect dominates and we expect a positive cross-correlation with foreground galaxies whereas for faint samples with a flatter count slope we expect a negative cross-correlation signal. Intermediate QSO samples give a null result. For example, Boyle et al. (1988) found significant anti-correlation on scales of $4'$ around galaxies

* E-mail:georgios.mountrichas@durham.ac.uk

Table 1. Number of $g < 21$ QSOs, $g < 21$ galaxies and the QSO and galaxy density for each area separately

<i>area</i>	1	2	3	4	5
QSOs	5,373	10,380	5,720	15,225	1,178
Galaxies	203,164	455,541	216,204	679,200	45,050
QSOs deg^{-2}	34.5	31.6	31.8	29.2	30.2
Galaxies deg^{-2}	1302	1386	1202	1303	1155

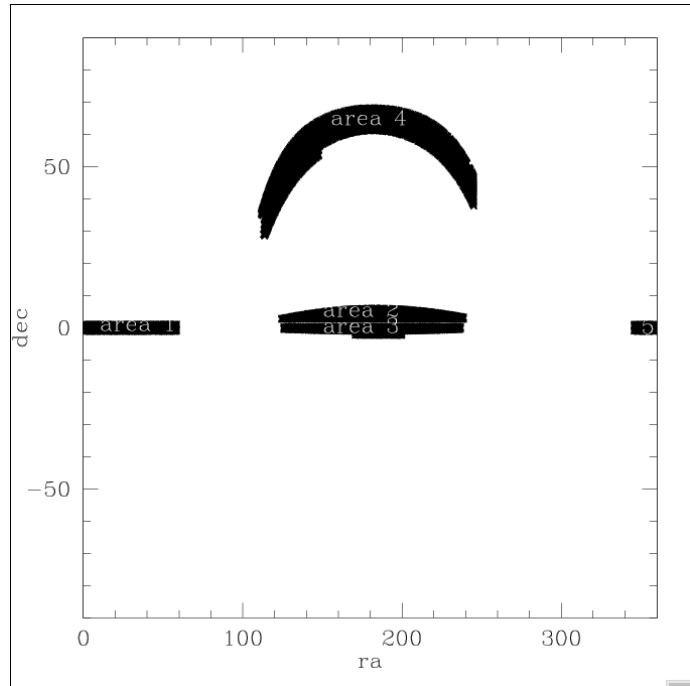
using faint QSOs ($B < 20.9$). Williams and Irwin (1998) and Nollenberg and Williams (2005) found significant positive correlation on angular scales of the order of one degree (their QSO samples respectively consisted of QSOs within $16 < m_B < 18.5$ and $13 < B < 17.5$) and Gaztanaga (2003) measured the cross-correlation between photometric galaxies and bright, $i < 18.8$ spectroscopic QSOs using only the SDSS EDR and found a positive cross-correlation of 20% on arcminute scales.

Although the idea seems simple, QSO-galaxy cross-correlations have been a controversial subject over the years as different results and different strength of the signal are detected even when the same or similar QSO magnitude samples have been used. In this paper we are looking for a possible explanation of the apparent discrepancy between the results of Scranton et al. (2005) and Myers et al. (2003, 2005) where in the latter papers they seem to find a much stronger anti-correlation signal at the same ($g < 21$) QSO magnitude limit. Our first aim will be to reanalyze the SDSS photo- z data and compare with previous results. In particular, we shall look for the effects of low redshift contamination in the photo- z QSO sample and also measure the QSO-galaxy cross-correlation at the same QSO and galaxy limits as used by Myers et al. (2003, 2005). We shall also be looking at the important effect of the $g < 21$ galaxy magnitude limit used by Myers et al (2003, 2005) as opposed to the $r < 21$ limit used by Scranton et al (2005).

In Section 2 we explain the data that we use and how they differ from Scranton et al. and Myers et al. (2005) data sets, as well as providing details of our analysis. In Section 3 we present our results from QSO-galaxy cross-correlation and in Section 4 the results of correlating the same QSOs with galaxy groups. In Section 5 we check the low- z galaxy/QSO contamination in Richards et al. QSO sample that we (and Scranton et al.) use and the effect of this contamination on the results. Note that we use the term contamination in different contexts to include both ‘catastrophic redshift failures’ and also non-QSOs in the $1 < z_p < 2.2$ QSO sample. In Section 6 we use fitting models for the cross-correlations with clusters and galaxies from Myers et al. (2003 and 2005) and Scranton et al and compare them with our results. Finally, in Section 7 we discuss the conclusions that can be drawn as to the reason that causes the difference in the results in the three published papers.

2 THE DATA AND ANALYSIS

Our galaxy sample consists of SDSS DR4 galaxies at the magnitude limit of $g \leq 21$ where the sky density is \simeq

**Figure 1.** The distribution of our QSO and galaxy samples. The numbers indicate the areas in which the samples were cross-correlated. Area 3 is the 2QZ area.

1200deg^{-2} . It should be noted at the outset that our galaxy sample and that of Myers et al. (2005) is different from that of Scranton et al., as they use galaxies with $r < 21$ with a sky density of $\simeq 3500 \text{deg}^{-2}$. This means that care must be taken in comparing these results because the projected galaxy clustering in the $r < 21$ sample will have $\approx 2 \times$ lower correlation function amplitude due to its increased depth. The QSO sample we use is the same sample which is extracted by Richards et al. (2004), by applying their ‘Kernel Density Estimation’ method on the DR1 dataset. Scranton et al. use a similar method to extract their QSO sample but they apply it to the DR3 set instead. We also use the same redshift range as Scranton et al. which is $1.0 \leq z_p \leq 2.2$. So the main difference between the QSO sample we use for our analysis and Scranton et al. use for theirs should be a larger number of QSOs in their sample (DR3 vs. DR1).

In total we have 37,876 QSOs in the above redshift range and 1,599,159 galaxies. The numbers for each area separately as well as the galaxy density ($g < 21$) are shown in Table 1. Our random catalogue consists of 7 times the number of the galaxies. All ‘holes’ found in SDSS data have been added to our random catalogues so the numbers shown above are our final number of objects. Fig. 1 shows the distribution of the QSOs that comprise our sample. The indicated areas 1-5 are those that were used for our cross-correlation analysis. In terms of our analyses of the SDSS photo- z QSO samples, we accept that these may be less sophisticated than those of Scranton et al. For example, we do not mask out poor seeing or high reddening areas and we use the standard SDSS star-galaxy classifier rather than Bayesian star-galaxy separation parameters. We believe that our $g < 21$ QSO limit is conservative enough to make these differences cause

negligible effects. More importantly, we ignore the statistical ranges allowed for QSO photo- z , z_p , generally taking a sharp cut with $1 < z_p < 2.2$. Scranton et al also weight their cross-correlation by the QSO photo- z probability. We shall flag the points where these different approaches may affect our conclusions.

The 2QZ QSOs are taken from the 2QZ catalogue (Croom et al. 2004). The 2QZ comprises two $5deg \times 75deg$ declination strips, one in an equatorial region in the North Galactic Cap (NGC) and one at the South Galactic Pole (SGC). In our analysis when we mention the 2QZ area or 2QZ QSOs we mean only the NGC of the 2dF QSO survey, unless we present results from Myers et al. (2005) in which case the cross-correlation has been done in both the NGC and SGC. We should underline here that the most important difference between the 2QZ and the DR1 QSO dataset that we use or the DR3 that Scranton et al. use is that 2QZ QSOs are spectroscopically confirmed whereas the method used to extract the DR1/DR3 QSOs is based on Bayesian photometric classification and the redshifts assigned to the objects are photometric redshifts.

Throughout our analysis we centre on QSOs and count galaxies or clusters for our cross-correlations so our random catalogues are constructed with the same angular selection function as our galaxy samples. To measure the two-point correlation function $\omega(\theta)$, we use the expression (Peebles 1980),

$$\omega(\theta) = \frac{DD_{12}(\theta)\bar{n}}{DR_{12}(\theta)} - 1 \quad (1)$$

where DD_{12} is the number of data-data point pairs (e.g. QSO-galaxy pairs) and DR_{12} is the data-random point pairs. \bar{n} is a factor which shows how many more random points than data points we have (7 in our case). Our errors are field-to-field errors (Myers et al., 2003). In this case we divide our data sets into 25 subsamples and measure the field-to-field variations of the cross-correlation function. The error is then estimated as the standard error inverse weighted by variance to account for different numbers of objects in each subsample, i.e.

$$\sigma_{\omega}^2(\theta) = \frac{1}{N-1} \sum_{L=1}^N \frac{DR_L(\theta)}{DR(\theta)} [\omega_L(\theta) - \omega(\theta)]^2 \quad (2)$$

Since 2QZ QSOs had higher priority than 2dFGRS galaxies for spectroscopic observations there is no issue for fibre incompleteness to deal with. Of course, this is also true for the photo- z sample. On the smallest scales there is a lower limit for cross-correlation of $10''$ due to confusion caused by galaxy overlaps.

3 QSO-GALAXY CROSS-CORRELATION RESULTS

We first cross-correlate our SDSS DR1 photo- z $g < 21$ QSO sample with our SDSS DR4 $g < 21$ galaxy sample. The results are shown in Fig. 2 by the black filled circles. For comparison the NGC results from Myers et al. (2005) have also been added (triangles) without their errorbars and for reference the results from Scranton et al. (squares) also without their errorbars. The results from Scranton et al. are

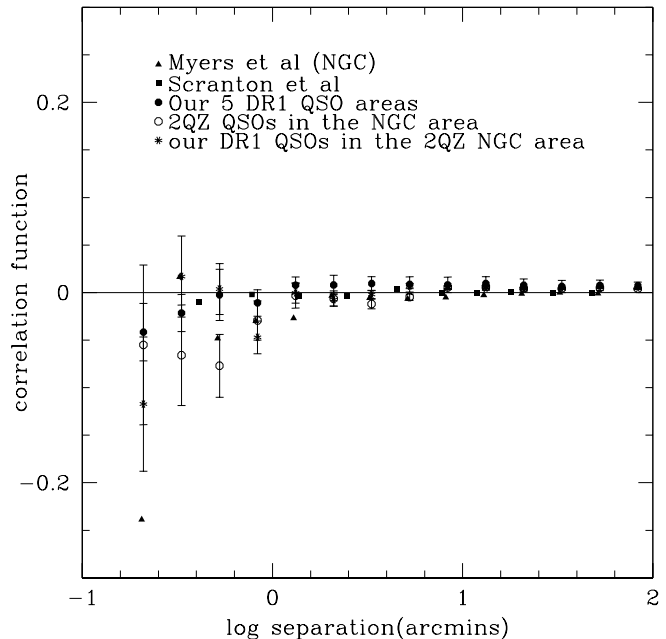


Figure 2. QSO-galaxy cross-correlation results. Our DR1 results are shown by the black filled circles and cover the whole magnitude range for the QSO sample ($g < 21$) and $g < 21$ for the galaxies. Triangles are the results from Myers et al. (2005) for the NGC of the 2QZ (centring on QSOs and counting galaxies). Squares show Scranton et al. where the faintest QSO sample has been used, $20.5 < g < 21$, and $r < 21$ for galaxies. We have also included our results by cross-correlating 2QZ QSOs with the same galaxy sample in the 2QZ area. These results are shown by the open circles. Asterisks show the results from cross-correlating our DR1 QSOs with the same galaxy sample in the 2QZ area. The errors are field-to-field errors.

taken from their faintest QSO sample $20.5 < g < 21$, cross-correlated with $r < 21$ galaxies. From this plot it seems that our results are slightly higher than those of Myers et al. (2005) throughout most of the range of scales. The Scranton et al. results have a smaller anti-correlation signal as expected due to the different galaxy sample they use (Section 6).

We have also included the results when we cross-correlate 2QZ QSOs with the same galaxy sample ($g < 21$) in the 2QZ NGC area. These results are shown by the open circles. This is $1.8 \times$ bigger area than used by Myers et al. (2003, 2005) due to the smaller SDSS area previously available. Finally, asterisks show the results from cross-correlating our DR1 QSOs with the same galaxy sample in the 2QZ area. The 2QZ QSOs again tend to give more anti-correlation than the DR1 QSOs cross-correlated with the same galaxy sample.

Fig. 3 shows the same results as the previous plot but this time our DR1 QSO sample consists of 17,426 QSOs with magnitude $20.5 \leq g \leq 21.0$. The amplitude of the anticorrelation signal is similar to that found in Fig. 2 for $g < 21$ QSOs and again is stronger, as expected, than the signal detected by Scranton et al. for $r < 21$ galaxies, but consistent with Myers et al.

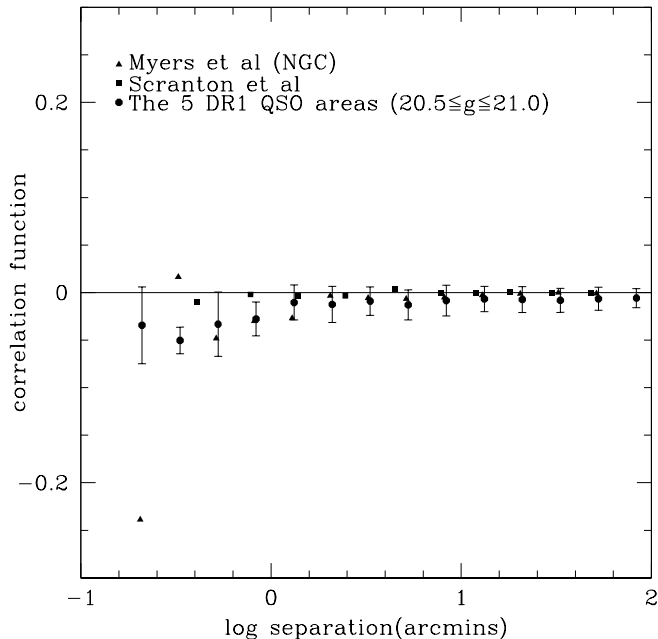


Figure 3. QSO-galaxy cross-correlation results. This time our DR1 QSO sample comprises of QSOs with $20.5 \leq g \leq 21.0$. The errors are field-to-field errors. Triangles are the results from Myers et al. (2005) and squares from Scranton et al.

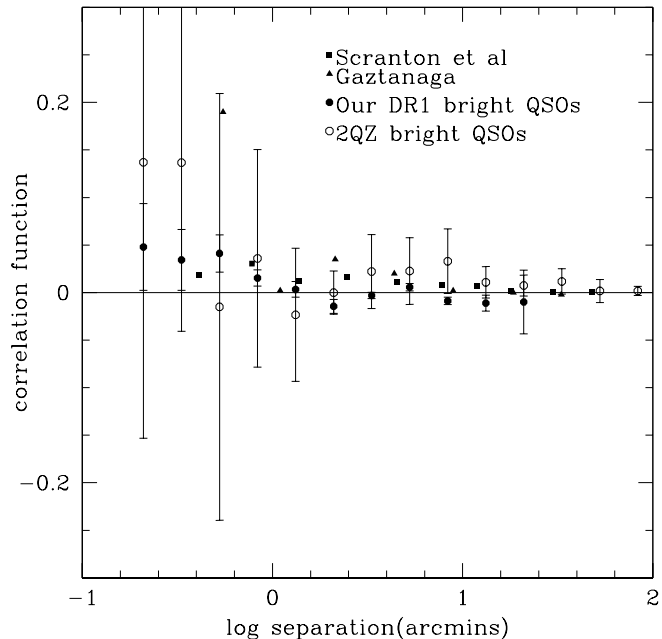


Figure 4. QSO-galaxy cross-correlation results for bright QSOs. Our DR1 QSO sample consists of QSOs with $17 \leq g \leq 19$ (black circles). The results of Scranton et al. for QSOs with $17 \leq g \leq 19$ and galaxies with $r < 21$ are also shown (squares). The triangles show the results from Gaztanaga (2004). His sample consists of QSOs with $18.3 \leq i \leq 18.8$ and $0.8 \leq z \leq 2.5$ and galaxies with $19 < r < 22$. Finally, we present the results from the 339 bright ($18.25 \leq b_j \leq 19.0$) 2QZ QSOs in the 2QZ area (open circles).

Fig. 4 shows the QSO-galaxy cross-correlation results for bright QSOs. Here our DR1 sample consists of $1.0 < z_p < 2.2$ QSOs in the magnitude range $17 \leq g \leq 19$, Scranton et al. (squares) where the QSOs have $17 \leq g \leq 19$ and the galaxies have $r < 21$. We have also plotted the results from Gaztanaga (2004) (triangles) where the specific data points are drawn from his QSO sample with $18.3 \leq i \leq 18.8$ and $0.8 \leq z \leq 2.5$ and their galaxy sample with $19 < r < 22$. We then show the results when we cross-correlate the 339 bright ($18.25 \leq g \leq 19.0$) 2QZ QSOs in the 2QZ NGC area (open circles). These results give zero signal and a bump appears on scales from $4' - 16'$. This bump is consistent with the statistical noise as we can see from the field-to-field error bars and moreover it disappears when we cross-correlate the same QSO sample with galaxies in groups (Section 4, Fig. 9). Our DR1 and 2QZ results seem consistent although the errors are large. Both results also appear lower than the results of Gaztanaga. The results are consistent with those of Scranton et al. although their galaxy sample is fainter. Summarising, our results for bright QSOs, from DR1 and 2QZ give, at least at small scales, a less positive cross-correlation than that seen by Gaztanaga but one consistent with that found by Scranton et al., although the S/N is poor. The interpretation of this latter result requires account to be taken of their fainter limit and the QSO count slope at $g \simeq 19$. We postpone further discussion to Sections 5 and 6 where the effects of contamination will also be discussed.

4 QSO-GALAXIES IN GROUPS CROSS-CORRELATION RESULTS

The next step was to find groups of galaxies in the 5 areas of the DR4 dataset. Although there are no group results from Scranton et al. with which to compare, we can still compare the QSO photo- z and spectroscopic results, in a situation where the S/N of any lensing effect may be expected to be higher than for galaxies. We therefore use the same method that is described in Myers et al. (2003) and references therein to determine these groups. We use a factor δ by which we wish our group density to exceed the mean surface density of the area that is being examined. In our case we use $\delta = 8$. Then we draw a circle with the largest possible radius, such that our group density doesn't fall below δ times the mean surface density. Groups are defined when these circles overlap and the mean surface density does not fall below the critical value (friends-of-friends). From these groups we select for our cross-correlations the ones with at least 7 members in order to reduce the likelihood of chance alignments of galaxies at different redshifts being grouped together. An example of how the galaxies of these groups look is shown in Fig. 5. In total there are 14,143 groups with more than 7 members in the 5 areas that we use.

We next cross-correlated our DR1 QSO sample with galaxies that are in groups with at least 7 members. The signal detected in this case is usually stronger than the one in QSO-galaxy cross-correlations because groups have a big-

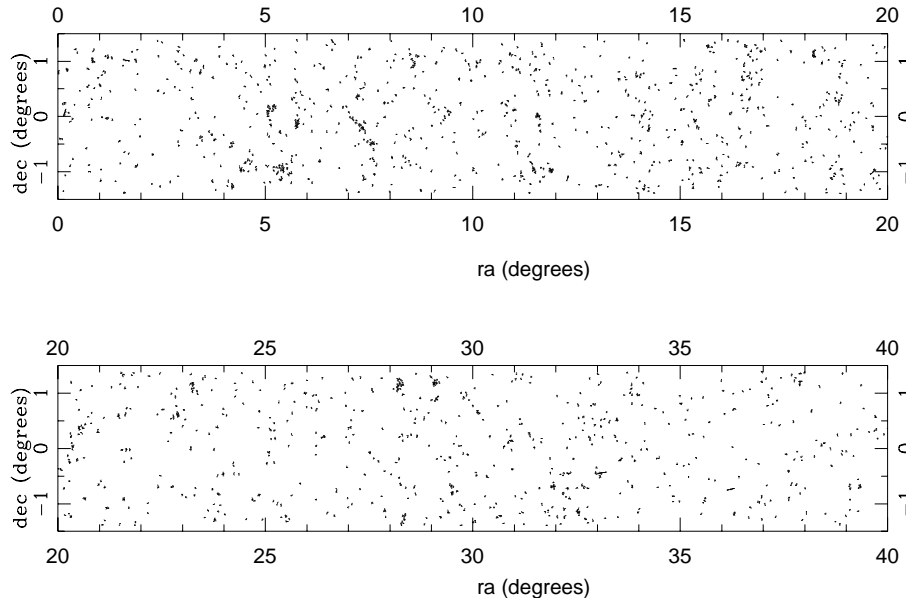


Figure 5. Galaxies ($g < 21$) in groups with more than 7 members in the strip between $-1.5 < \delta < +1.5$ deg and $0h < \alpha < 2h40$ in Area 1.

ger mass. In total our galaxy sample consists of 146,490 galaxies in groups. In Fig. 6 we show the results for each of the 5 areas separately. The errors are field-field errors. An anti-correlation effect is consistently seen in all 5 areas. The combined results for all the 5 areas are shown in Fig. 7. For comparison, the results from Myers et al. (2003) for both the NGC and SGC have been added (triangles). They use 22,417 2QZ QSOs and nearly 300,000 galaxies of limiting magnitude $b = 20.5$ found in groups of at least 7 members. From the comparison we see that their signal is stronger on scales of 0.4-2.5 arcmins, which is expected as the results from the SGC show a slightly stronger anti-correlation signal (Myers et al., 2003) and so they push the overall result down. Again, as for the QSO-galaxy results we show the results of the cross-correlation of 2QZ QSOs with the galaxies in clusters in the NGC of the 2QZ area. The results are shown by the open circles. Finally, asterisks show the results from our DR1 QSO cross-correlation with the same galaxy sample in the 2QZ area. The signal detected is at a lower level. From the plot we see that 2QZ QSOs give a stronger anti-correlation signal than the one detected by using our DR1 QSOs in the 2QZ area but statistically consistent with Myers et al (2003).

Previously we have cross-correlated individual group galaxies rather than the centre of groups. Fig. 8 shows the

results from DR1 QSOs with centres of groups of galaxies with more than 7 members (filled circles). Open circles show the results from Myers et al. (2003) combined for both the NGC and the SGC together with a best fit model which will be briefly discussed in Section 7. Although these results are generally easier to compare directly with models, the signal-noise is weaker due to non-weighting by cluster membership. Again our DR1 results appear to show less anti-correlation than the 2QZ results.

Fig. 9 also shows the results from cross-correlating our bright DR1 QSOs ($17.0 \leq g \leq 19.0$) with galaxies in clusters with more than 7 members (filled circles). Some positive signal at $1'$ is again seen, increased by about a factor of four from the QSO-galaxy case in Fig. 4. However, the positive signal is still only at a marginally significant level. We shall argue later that the lack of a strong positive signal may be explained by being close to the knee of the QSO count slope where $\beta \approx 0.4$ and only a small lensing effect might be expected.

Finally, we extracted the bright QSOs from the 2QZ sample ($18.25 \leq b_j \leq 19.0$, $1.0 \leq z \leq 2.2$) and cross-correlate them with galaxies in clusters (with more than 7 members). The results are shown by the open circles in Fig. 9 and seem to give a slightly positive signal but this result is again not statistically significant. Also, the bump

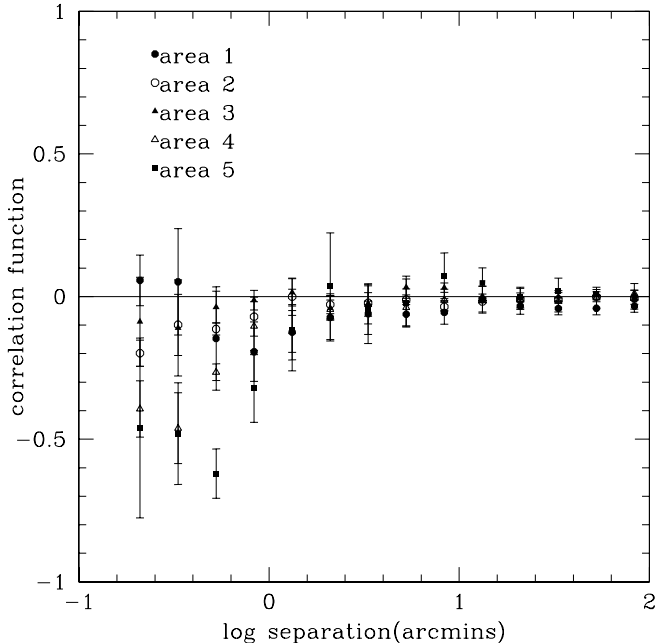


Figure 6. The DR1 QSO - DR4 galaxies in groups cross-correlation results for each area separately. The errors are field-to-field errors.

that appeared in Fig. 4 when we cross-correlated the same QSO sample with galaxies has disappeared.

5 CONTAMINATION IN THE QSO SAMPLE

As previously noted our DR1 QSO sample consists of photometric QSOs that are derived using the method described by Richards et al. and is similar to the method that has been used by Scranton et al. The main difference with the Scranton et al. sample is that their sample is extracted from DR3 whereas the sample we use is extracted from DR1. In this Section we examine the contamination percentage in our photometric sample and how this contamination could change the results. The contamination that is most important is the fraction of low redshift QSOs and compact narrow emission-line galaxies (NELGs) in the $1.0 < z_p < 2.2$ QSO photo- z sample since they can confuse any lensing signal with intrinsic clustering with the galaxies but we shall also include stellar contamination which can dilute to a lesser extent the lensing signal. Richards et al. (2004) and also Myers et al (2007) claim 5% non-QSO contamination over the full magnitude and redshift range. We now wish to check this number and, more importantly, also determine the contamination of the $1 < z_p < 2.2$ QSO photo- z sample by $z < 0.6$ ($z < 0.3$) QSOs and NELGs that may affect cross-correlation with $r < 21$ ($g < 21$) galaxies.

5.1 Comparison with the 2QZ catalogue

In order to check the contamination in the DR1 QSO sample we first compare it with the 2QZ catalogue. In the 2QZ

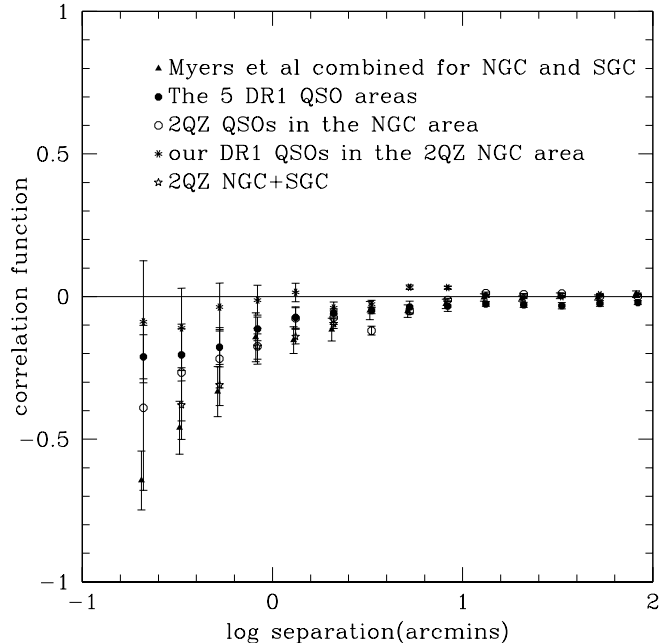


Figure 7. Cross-correlation between QSOs and galaxies in groups of galaxies with at least 7 members (filled circles). The errors are field-to-field errors. The triangles show the combined results from Myers et al. (2003) for both the NGC and SGC. They use 22,417 2QZ QSOs and nearly 300,000 galaxies of limiting magnitude $b = 20.5$ found in groups of at least 7 members. Their cross-correlation is done in the SGC and NGC strip of the 2QZ. From the comparison we see that their signal is stronger on scales of 0.4-2.5 arcmins. We also show the results of the cross-correlation of 2QZ QSOs with the galaxies in clusters in the 2QZ area. The results are shown by the open circles and give a weaker anti-correlation signal than found in the results of Myers et al. but still the signal is stronger than the one detected by using our DR1 QSO sample. Asterisks show the results from our DR1 QSOs cross-correlation with the same galaxy sample in the 2QZ area. Stars show the results when we average our open blue circles from the NGC of 2QZ with Myers et al. results for the SGC.

there are 23,290 objects and in our DR1 QSO sample 4,535 QSOs in the 2QZ area, with $g < 20.85$, $1.0 < z < 2.2$. 3,025 objects are common in the two sets. 2,516 of these objects have been identified as QSOs in the 2QZ and 509 have different or no ID in the 2QZ, ie 16 are NELGs, 91 stars and 402 have not been identified by the 2QZ team. Finally, 1,510 ($= 4,535 - 3,025$) DR1 QSOs are not included in the 2QZ. The contamination in this case refers to objects that have been identified as QSOs in our DR1 photometric sample but have different IDs in the 2QZ catalogue and QSOs that have been assigned a high photometric redshift but their spectroscopic redshift in the 2QZ data set is lower. Fig. 10 shows the photometric vs. the spectroscopic redshift of the common objects (including stars, NELGs and objects with no ID). Table 2 summarises the contamination statistics as derived from the plot. There are 169 low spectroscopic redshift QSOs and NELGs in a total of 2024 objects. According to these numbers we find a contamination of $(8.3 \pm 0.6)\%$ for objects that have photometric redshift between $1.0 < z_p < 2.2$ and

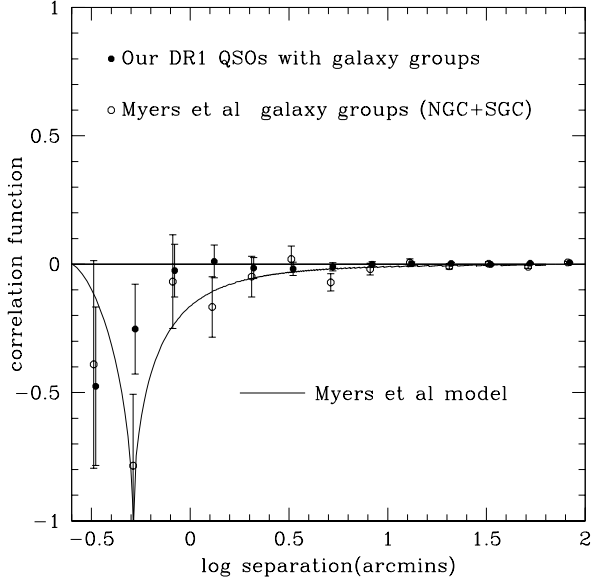


Figure 8. Cross-correlation between DR1 QSOs in 5 areas and centres of groups of galaxies with at least 7 members, assuming $\delta = 8$. Open circles show the results from Myers et al. (2003) combined for both the NGC and the SGC together with a best fit model which will be briefly discussed in Section 8. Our signal here is less strong due to non-weighting by cluster membership.

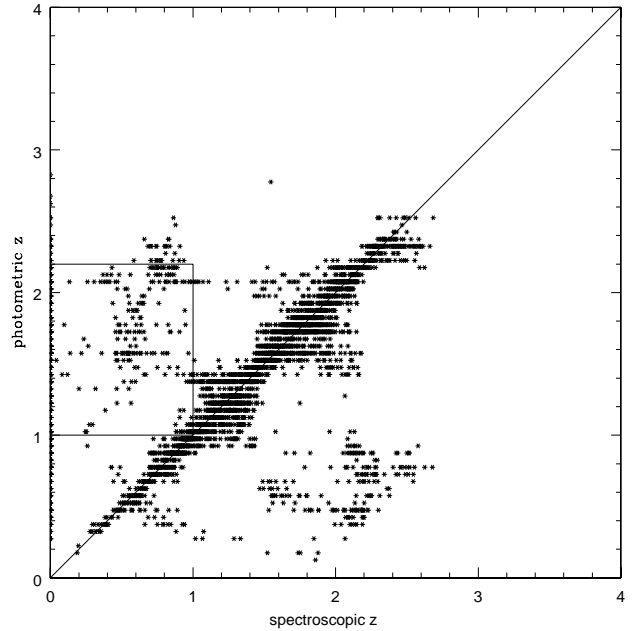


Figure 10. Photometric vs. spectroscopic redshift for the common objects between the DR1 and 2QZ catalogues.

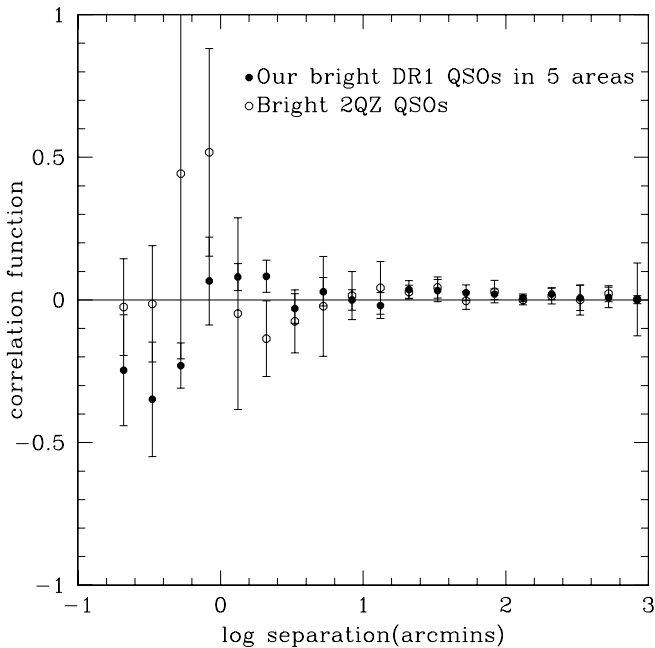


Figure 9. Bright 2QZ QSOs ($18.25 \leq b_j \leq 19.0$, $1.0 \leq z \leq 2.2$) cross-correlated with galaxies in clusters with at least 7 members (open circles) give a slightly stronger positive signal but still insignificant. Also, the bump has disappeared which suggests that it was due to statistics. Filled circles show the results for our bright DR1 QSOs ($17.0 \leq g \leq 19.0$) cross-correlated with galaxies in clusters with at least 7 members in the 5 areas. A signal is marginally detected at $1'$.

2QZ spectroscopic redshift $z_s < 1.0$. In the same way the contamination of spectroscopic redshift $z_s < 0.6$ objects is $(3.6 \pm 0.4)\%$ (73 low spectroscopic redshift QSOs and NELGs in a total of 2,024 objects). Finally, for $z < 0.3$ the contamination is $(0.6 \pm 0.2)\%$ (12 spectroscopic redshift QSOs and NELGs at low- z in a total of 2,024 objects).

DR1 objects that have been identified as stars in the 2QZ also dilute any anti-correlation by the factor $(1 - f_s)^2$ where f_s is the fraction of stars in the the DR1 sample. This effect of including uncorrelated stars is usually much smaller than the effect of including low redshift NELGs and QSOs. From Table 2 $f_s = 55/2024 = 2.7\%$ giving $(1 - f_s)^2 = 0.95$ which implies that the anti-correlation is also decreased by $\approx 5\%$ due to star contamination.

5.2 Comparison with the 2QZ+SDSS catalogue

The DR1 QSO catalogue we are using has also spectroscopic redshifts for the QSOs wherever available, either from the 2QZ or from spectra obtained by SDSS. Based on this information there are 1,215 NELGs and QSOs with photometric redshift $1.0 < z < 2.2$ and spectroscopic redshift $z < 1.0$ out of 15,776 objects. So the overall contamination is $(7.7 \pm 0.2)\%$. For spectroscopic redshift $z < 0.6$ there are 594 contaminating QSOs and NELGs so the contamination is now $(3.8 \pm 0.2)\%$ and finally for $z < 0.3$ there are 134 low spectroscopic QSOs and NELGs and the contamination is $(0.9 \pm 0.1)\%$. At $20.5 < g < 21$ 39/936 are $z < 0.6$ QSOs and NELGs and so the contamination here is $4.2 \pm 0.7\%$

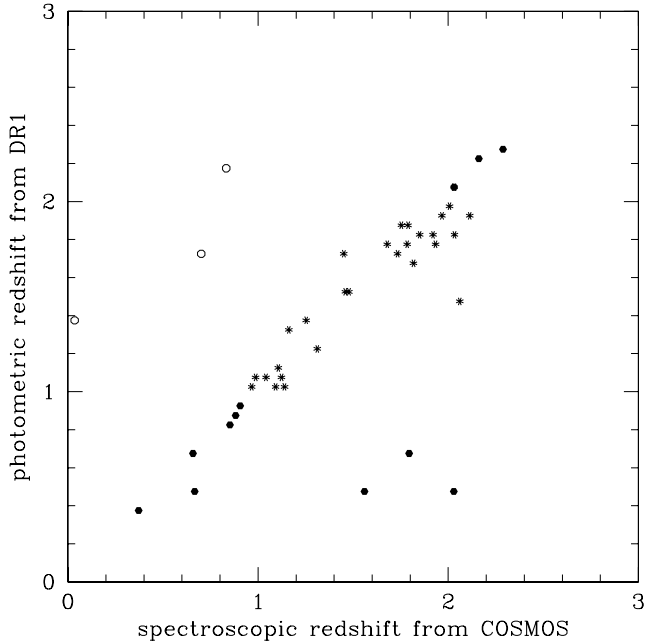


Figure 11. Spectroscopic redshifts (from Prescott et al.) against photometric redshifts (from DR1 sample). The open circles are the three contaminants and the asterisks are the objects with photometric redshift $1.0 < z < 2.2$.

5.3 Comparison with QSOs in the COSMOS field

Next we repeated the same procedure using the QSO spectroscopic sample from the Prescott et al. (2006). In that paper they confirm 95 quasars from the SDSS DR1 catalog in the COSMOS field. The quasars are within $18.3 < g < 22.5$ and a range in redshift $0.2 < z < 2.3$. 42 out of these 95 QSOs are in our DR1 sample at its $g < 21$ limit and 31 have $1.0 < z_p < 2.2$. So in a similar way we plot their spectroscopic redshift (from Prescott et al.) against their photometric redshift (from our DR1 sample) in Fig. 11. As we see there are three contaminants (open circles) out of the 31 objects that have photometric redshift between $1 < z_p < 2.2$ (asterisks), so the contamination now is $(9.7 \pm 5.6)\%$ with spectroscopic redshift $z < 1.0$. Only one of these 3 has $z < 0.6$ and this has $z = 0.0375$ which makes the contamination $(3.2 \pm 3.2)\%$ both for spectroscopic redshift ranges $z < 0.6$ and $z < 0.3$ but the sample may be too small to draw any strong conclusion.

5.4 Comparison with spectroscopic QSOs from AAΩ.

In order to check the contamination statistics particularly of the $\approx \frac{1}{3}$ DR1 QSOs that lie outside the 2QZ selection at $g < 21$ we made new AAΩ (Sharp et al. 2006) observations in four fields. A full description of the observations will be given by Mountrichas et al (2007) so they are described only briefly here. The AAΩ fields are the COSMOS field with centre 10 00 28.8 02 12 21, the COMBO-17 S11 field with 11 42 58.0 -01 42 50, the 2SLAQ d05 field with

13 21 36.0 -00 12 35 and the 2SLAQ e04 field 14 47 36.0 -00 12 35. There are 123 QSO spectra taken for DR1 QSOs that are not previously included in 2QZ nor in COSMOS. In the data reduction we used the AUTOZ and 2DFEM-LINES routines written by Lance Miller and Scott Croom for the 2QZ. We first used AUTOZ which automatically identifies objects and assigns redshifts to them. Then, using the 2DFEM-LINES program we checked these redshifts by eye. This program steps through each object in the file created by the AUTOZ in turn starting with the best IDs through the worst. If the ID and the redshift are ok we moved to the next object. If either the identification or the redshift were not secure a ‘?’ quality flag was put next to the ID or the redshift. From these 123 objects identified as QSOs in our DR1 QSO photometric sample there were 5 NELGs with $z \leq 0.3$ and 1 QSO with $z < 0.6$. So from the comparison of our photometric sample with this spectroscopic one, the contamination is $(4.1 \pm 1.8)\%$ for $z \leq 0.3$ and $(4.9 \pm 2.0)\%$ for $z \leq 0.6$. For these calculations we have only taken into account first-class spectra that have unambiguous redshifts. That means that whenever we had to add a question mark to the redshift then this object was excluded as a potential contaminant but was still counted in the 123 objects. If we exclude these objects as well from the total number of objects, then the total number of good spectra falls to 78 and the contamination goes up to $(6.4 \pm 2.9)\%$ for $z \leq 0.3$ and $(7.7 \pm 3.4)\%$ for $z \leq 0.5$. The former, more conservative, numbers are listed in Table 3.

5.5 Summary of the contamination results

The contamination results summarised in Table 3 allow comparison between the three data sets described above. From that we can conclude that for spectroscopic redshift $z < 0.3$ our DR1 sample has an $\approx 2\%$ contamination. This comes from the fact that $1/3$ of our sample which is in 2QZ has contamination 0.6% and the rest has $4.1 \pm 1.8\%$ as found from the comparison with the four AAΩ fields. Weighting by the relative size of the 2QZ and non-2QZ components of the DR1 $1 < z_p < 2.2$ QSO sample, this gives an estimate of $1.8 \pm 0.6\%$ for the $z < 0.3$ contamination. The error here is dominated by the AAΩ estimate of the non-2QZ DR1 contamination. However, we note that the 2QZ+SDSS contamination is higher ($0.9 \pm 0.1\%$) than the 2QZ contamination ($0.6 \pm 0.2\%$) and that the COSMOS estimate of overall contamination is also higher so we believe our estimate of $1.8 \pm 0.6\%$ for $z < 0.3$ contamination is reasonable. The DR1 $z < 0.6$ contamination, which is more appropriate for $r < 21$ selected galaxies, is similarly estimated to be $(2/3 \times 3.6 + 1/3 \times 4.9) = 4.0 \pm 0.7\%$ (see Table 3). The overall contamination for $z_s < 1$ is estimated to be $(2/3 \times 8.3 + 1/3 \times 10.6) = 9.1 \pm 0.6\%$. This can be compared to the low-redshift contamination rate of 7.3% (A.D. Myers, priv. comm) indicated by Fig. 2 of Myers et al. (2007). These contamination fractions may only apply approximately to the QSO-photo-z sample of Scranton et al since a more detailed comparison would need to take account of their use of the statistical redshift range allowed by the photo-z estimates.

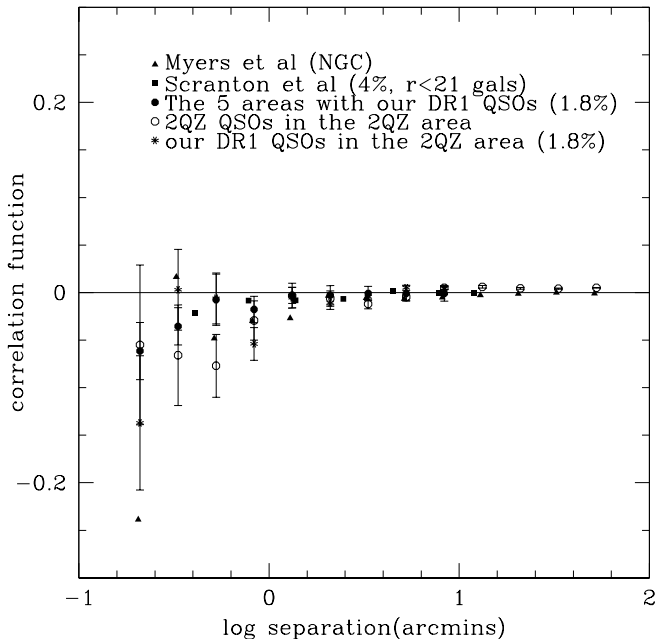


Figure 12. QSO-galaxy cross-correlation results as in Fig. 2 but our DR1 QSOs in the 5 areas (filled circles) and in the 2QZ area (asterisks) have been changed assuming contamination of 1.8% and the fit to $g < 21$ galaxy autocorrelation function shown in Fig. 17. Scranton et al. (squares) have also been changed assuming contamination of 4% and the fit to the $r < 21$ galaxy autocorrelation function (Fig. 17).

5.6 Effects of $\simeq 2\%$ contamination on the DR1 QSO-galaxy results

Now we shall see how an $\approx 2\%$ contamination for $z \leq 0.3$ can alter our cross-correlation results in the case of QSO-galaxy and QSO-cluster cross-correlations. We will first base our calculations on the galaxy-galaxy autocorrelation results at $g \leq 21.0$ represented by $w = 0.33\theta^{-0.8}$ with θ in arcmins (see Fig. 8 of Myers et al). We multiplied this $g < 21$ galaxy $w(\theta)$ by the $z < 0.3$ 1.8% contamination estimate, and then subtracted this correction from the SDSS photo- z galaxy-QSO cross-correlation results. At $1'$ this correction is -0.007 and at the smallest bin $\theta = 0'.2$ the correction only rises to -0.02.

Assuming this correction, our previous Fig. 2 now appears as seen in Fig. 12. In this plot our DR1 QSO results in the 5 areas (filled circles) have been changed assuming 1.8% contamination and remain statistically consistent with the 2QZ QSO results (open circles). The agreement improves but only slightly. Also, the results using our DR1 QSO sample in the 2QZ area (asterisks) have been changed using the same corrections and they remain statistically consistent with the 2QZ QSO and our DR1 QSO results.

Finally, we have corrected the Scranton et al. results (squares) assuming contamination of 4% and the fit to the $r < 21$ galaxy autocorrelation function shown in Fig. 17. At $1'$ this correction is -0.006 and at the smallest bin $\theta = 0'.3$ the correction rises to -0.01. The anti-correlation at $\theta = 0'.3$ increased by a factor of $\simeq 2$.

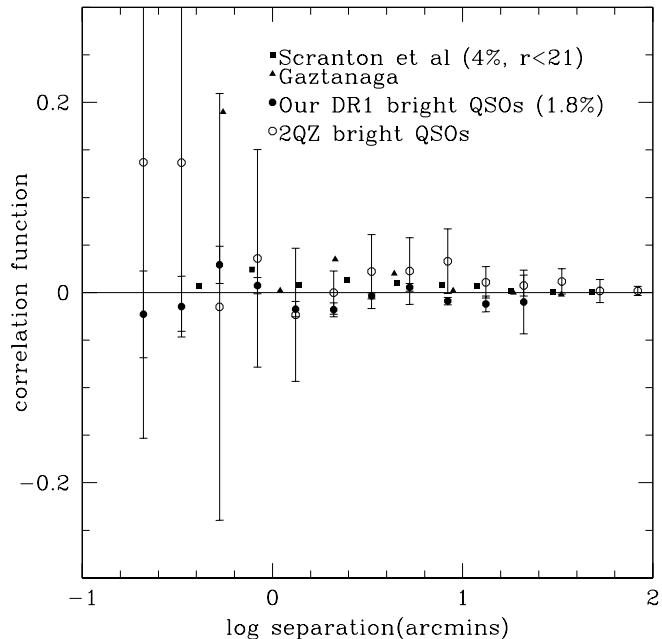


Figure 13. QSO-galaxy cross-correlation results for bright QSOs as in Fig. 4. Our DR1 QSO sample consists of QSOs with $17 \leq g \leq 19$ (filled circles) and is corrected assuming 1.8% contamination of the $g < 21$ galaxies, Scranton et al. (squares) is corrected assuming 4% contamination and the fit to the $r < 21$ galaxy autocorrelation function shown in Fig. 17. The triangles show the results from Gaztanaga (2004). His sample consists of QSOs with $18.3 \leq i \leq 18.8$ and $0.8 \leq z \leq 2.5$. Finally, we present the results from the 339 bright ($18.25 \leq b_j \leq 19.0$) 2QZ QSOs in the 2QZ area (open circles).

We have also corrected the results for the bright photo- z QSOs samples that appear in Fig. 4. The corrected results are shown in Fig. 13 assuming 1.8% contamination. These results show some positive signal but only at marginally significant levels. The most significant result is from the $17 < g < 19$ QSO-galaxy result of Scranton et al. which after correction gives $w_{qg} = 0.024 \pm 0.018$ at $1'$.

We now correct the QSO-cluster cross-correlations for contamination. Here we base the correction on the galaxy-cluster cross-correlation results of Stevenson et al. (1988) who used the same group detection parameters as we do here. They cross-correlate galaxies with groups of galaxies with > 7 and more than > 15 members down to $b_j = 20.2$ (see their Fig. 9). We use their results for clusters with more than 7 members which matches our cluster selection and we correct our results assuming as before 1.8% contamination of galaxies in our DR1 QSO sample. At $1'$ this correction is -0.11 and at the smallest bin $\theta = 0'.3$ the correction rises to -0.12. The results are shown in Fig. 14. Applying the 1.8% contamination correction to our results increases the anti-correlation at $1'$ by a factor $\simeq 3$ and improves consistency with the Myers et al. (2003) model at all scales.

Summarising, the effects of contamination are low for the photo- z QSOs when cross-correlated with $g < 21$ galaxy samples. They can be more significant at small scales for photo- z QSOs cross-correlated with $r < 21$ galaxy samples.

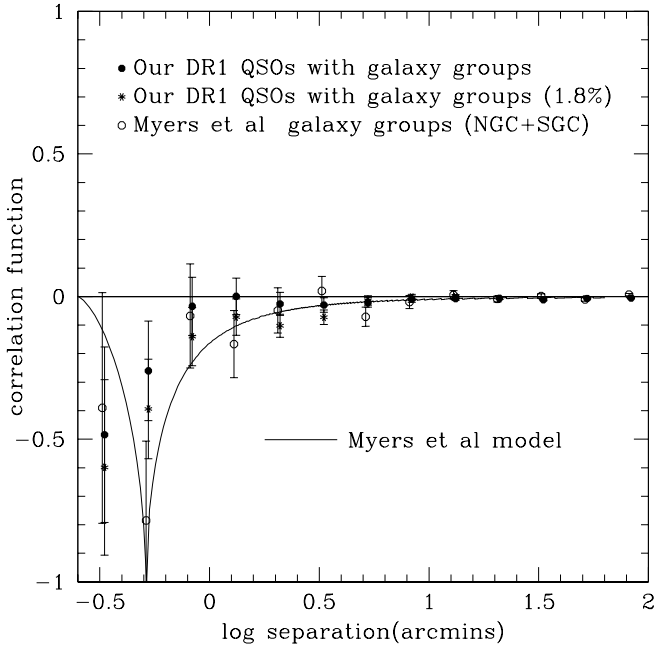


Figure 14. QSO-galaxy group centres cross-correlations. The filled circles show the QSO-group centres cross-correlation results as shown in Fig. 9. The asterisks show the results when we consider 1.8% contamination and take into account the galaxy-cluster results from Stevenson et al. Open circles show the results of Myers et al. (2003). The model from Myers et al. is also shown (solid line)

5.7 Contamination correction estimated via low-*z* objects in the 2QZ catalogue

A different way to correct for the contamination in the cross-correlation results is to base our correction on a cross-correlation between all the low redshift ($z \leq 0.6$) objects that are in the 2QZ catalogue (QSOs, NELGs, LINERs, ...) with the foreground galaxies. We found 2,667 low- z objects in the NGC of the 2QZ and the cross-correlation results with $g < 21$ galaxies appear in Fig. 15. Note that this result has a much lower amplitude than the $g < 21$ galaxy auto-correlation results due to the bigger mis-match between the average redshift of the $g < 21$ and $z < 0.6$ 2QZ samples. For the $g < 21$ galaxy results this cross-correlation correction used is similarly small to the auto-correlation corrections discussed above and so we only focus on the correction for the $r < 21$ galaxies of Scranton et al. We again use the 4% $z < 0.6$ contamination correction appropriate for $g < 21$ QSOs cross-correlated with $r < 21$ galaxies. The results are shown in Fig. 16 alongside the uncorrected results and the observational model ($\omega_{qg(\theta)} = -0.024 \pm_{0.007}^{0.008} \theta^{-1.0 \pm 0.3}$) from Myers et al. (2005). At $1'$ the correction is -0.0028 and at $\theta = 0'.3$ the correction is -0.004. So at $1'$ the auto-correlation function route gives a $2\times$ lower correction than the cross-correlation route. Since the $r < 21$ cross-correlation has poorer signal to noise while the autocorrelation route has more uncertainty associated with the assumed $n(z)$ in what follows we shall be using the average of these two corrections

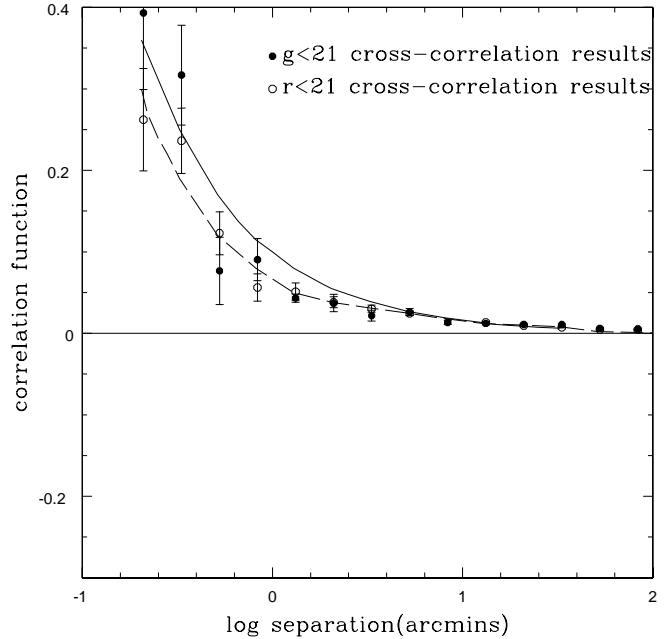


Figure 15. Cross-correlation of the 2,667 low redshift ($z < 0.6$) QSOs and NELGs in the NGC of the 2QZ with our $g < 21$ galaxy sample is shown by the filled circles. The line shows the best fit which is $w=0.11\theta^{-0.8}$. cross-correlation of the 2,667 low redshift ($z < 0.6$) QSOs and NELGs in the NGC of the 2QZ with our $r < 21$ galaxy sample is shown by the open circles. The dashed line shows the best fit which is $w=0.07\theta^{-0.8}$.

Table 2. CONTAMINATION. DR1 vs. 2QZ

object ID	$1.0 \leq z_p \leq 2.2, z_s \leq 1.0$	$1.0 \leq z_p \leq 2.2$
QSOs '11'	144	1999
NELGs	25	25
Stars '11'	55	55
Total number	224	2079
Contamination=	$169/2024 = (8.3 \pm 0.6)\%$	

for the QSO-galaxy cross-correlations of Scranton et al. The (average) corrected results are also shown in Fig. 16.

6 2QZ VERSUS SDSS COMPARISON - INCLUDING EFFECT OF THE GALAXY SAMPLES

As noted in Section 2 throughout our analysis we are using $g < 21$ galaxies whereas Scranton et. al use $r < 21$ galaxies. This is the reason (apart from the contamination of the photometric QSOs) that we don't expect to get the same answers for the QSO-galaxy cross-correlations. In Fig. 17 we show our auto-correlation results from $g < 21$ galaxies and the results from $r < 21$ galaxies. The galaxy auto-correlation for $g < 21$ is taken from Myers et. al (2005); the

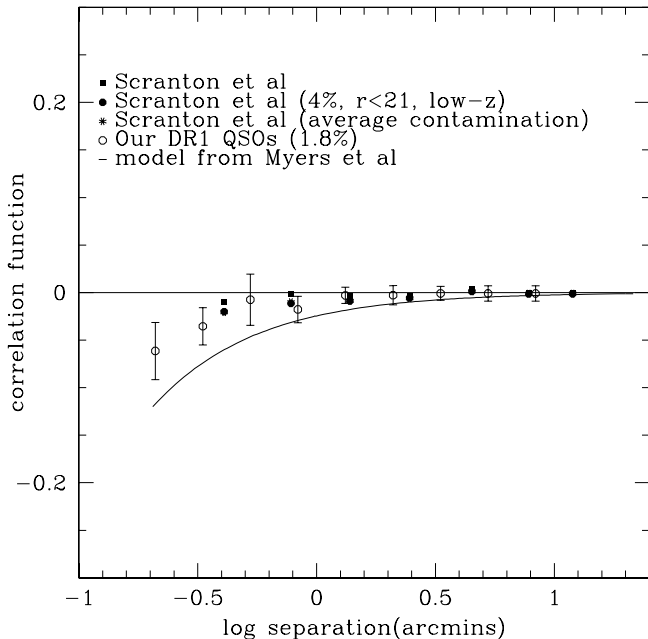


Figure 16. QSO-galaxy cross-correlation results. Squares show original Scranton et al. results, asterisks Scranton et al. assuming 4% contamination and the fit to the cross-correlation from the low redshift objects with $r < 21$ galaxies. Open circles show our DR1 QSOs when we apply 4% contamination and the fit to the cross-correlation from the low redshift objects with $g < 21$ galaxies. Filled circles show the results from the average of the two ways of estimating the contamination (galaxy auto-correlation and low- z objects) applied to Scranton et al. Finally, the line shows the Myers et al. (2005) model for QSO-galaxy cross-correlation.

Table 3. Summary of the contamination results

$1.0 \leq z_p \leq 2.2$	$z_s < 1.0$	$z_s < 0.6$	$z_s < 0.3$
2QZ set	$8.3 \pm 0.6\%$	$3.6 \pm 0.4\%$	$0.6 \pm 0.2\%$
2QZ+SDSS	$7.7 \pm 0.2\%$	$3.8 \pm 0.2\%$	$0.9 \pm 0.1\%$
COSMOS	$9.7 \pm 5.6\%$	$3.2 \pm 3.2\%$	$3.2 \pm 3.2\%$
4 $AA\Omega$ fields	$10.6 \pm 2.9\%$	$4.9 \pm 2.0\%$	$4.1 \pm 1.8\%$
Total	$\frac{2}{3}8.3\% + \frac{1}{3}10.6\%$	$\frac{2}{3}3.6\% + \frac{1}{3}4.9\%$	$\frac{2}{3}0.6\% + \frac{1}{3}4.1\%$
cont.=	$9.1 \pm 0.6\%$	$4.0 \pm 0.7\%$	$=1.8 \pm 0.6\%$

result for $r < 21$ has been calculated for 35000 SDSS galaxies to this limit. As we see there is a factor of 2-3 lower anti-correlation for the $r < 21$ galaxies. This is due to increased effects of projection on clustering in the $r < 21$ galaxy sample with its 50% increased depth and $3.5\times$ higher sky density (3500deg^{-2} vs. 1000deg^{-2}) which leads to weaker clustering. Therefore we also expect lower lensing anti-correlation signal by a similar factor of 2-3, based at least on the models used by Myers et. al (2005) from either Williams & Irwin (1999) or Gaztanaga (2004). Using $b \approx 0.1$ in a standard Λ CDM cosmology we predict the QSO-galaxy cross-correlation result for Myers et al. for galaxies with $r < 21$

($w_{qg}(r < 21) = \frac{A_{qg}(r < 21)}{A_{qg}(g < 21)}w_{qg}(g < 21)$ where A_{qg} is the amplitude of the galaxy auto-correlation function). The results are shown in Fig. 18. Squares show the Scranton et. al results (4% contamination averaged as described in Section 5.7) and the triangles show Myers et. al results renormalised for an $r < 21$ galaxy sample as described above. As we see the results are in very good agreement. So the disagreement between the Scranton et al. and Myers et al results is due to these two factors; contamination was not taken into account by Scranton et al. and the galaxy samples in the two analyses are different. When the results are changed based on those two factors they are consistent.

As already noted, the low signal seen in the corrected cross-correlation results for bright galaxies could very well be explained by the slope of the QSO number counts in the region of interest. Table 1 of Scranton et al (see also Myers et al., 2003) shows the slopes measured for the DR1 sample. At $19 < g < 19.5$ the slope is $\beta = +0.56$ and at $19.5 < g < 20.0$ the slope is $\beta = 0.43$. From equation (A5) of Myers et al. the magnification implied for groups by the anti-correlation of $w_{qg} \simeq -0.15$ at a QSO limit of $g < 21$ is $\simeq 0.5$ mag for groups at separation of $1'$ (see Fig. 14). Assuming the former $\beta = 0.56$ slope this would imply $w_{qc} \simeq 0.2$ for the $g < 19$ QSO-group correlation in Fig. 9. Assuming the latter $\beta = -0.43$ slope would imply $w_{qc} = 0.04$. This is consistent with the results shown in Fig. 9 at $1'$ where the contamination corrected $w_{qc} = 0.06 \pm 0.06$. The w_{qg} result of Scranton et al. at $17 < g < 19$ seems to show higher S/N than any of the others. If the contamination corrections obtained via Fig. 17 are the same as for the fainter samples, these results will only be slightly affected, decreasing from $w_{qg} = 0.02$ to $w_{qg} = 0.018$ on $1'$ scales.

The contamination corrected results from Scranton et al. for $17 < g < 19$ QSOs cross-correlated with $r < 21$ galaxies give $w_{qg} = 0.014 \pm 0.009$. If we take $w_{qg} = -0.01$ for $g < 21$ QSOs and the $r < 21$ galaxies then assuming $\beta = 0.29$ at $g < 21$ and $\beta = 0.564$ at $g \simeq 19$ this implies $w = 0.015$ from equation (A5) of Myers et al. (2003) and therefore the bright and faint results are in agreement, confirming the claim by Scranton et al. even after contamination correction.

In summary, the bright QSO-group galaxy correlation shows positive signal which is only slightly above the noise but is consistent with the anticorrelation signal at fainter magnitudes. From here on, we shall only model the faint QSO cross-correlation where the S/N is generally higher.

In a further paper we shall cross-correlate the SDSS spectroscopic QSOs at even brighter limits than discussed here to see if we can detect the positive correlation expected on the very steep part of the QSO number counts.

7 GALAXY MODEL FITTING

Since the observational results appear to be in agreement, the question then remains as to how the interpretations are so different. Scranton et al claim that a standard Λ CDM model can explain the QSO lensing data whereas Myers et al. suggest that $b \approx 0.1$ or a high mass density EdS cosmology (or both) is needed to explain the observations. Scranton et al. follow the Press-Schechter formalism of Jain, Scranton and Sheth (2003) assuming the standard cosmology and using the HOD prescription of Zehavi et al. (2005) as fitted

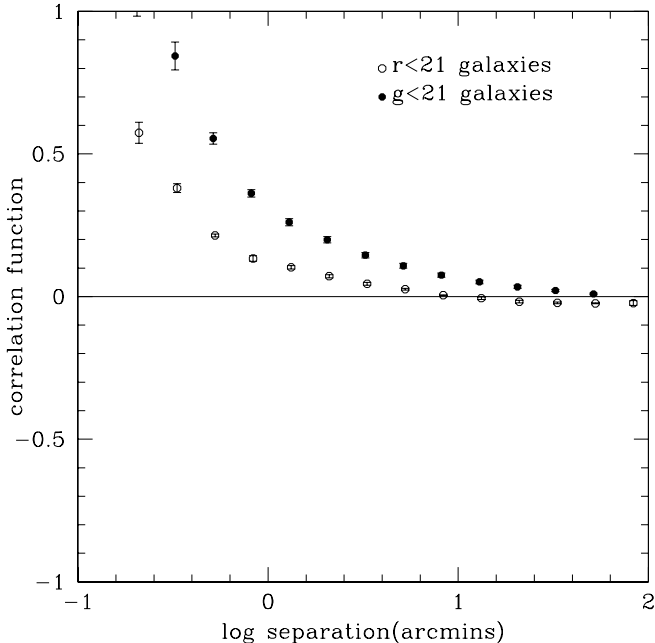


Figure 17. Galaxy auto-correlation results. The filled circles show the results from the $g < 21$ sample taken from Myers et al. (2005). Error bars represent 1σ jackknife errors. The open circles show the auto-correlation results for the $r < 21$ sample. The errors are field-field.

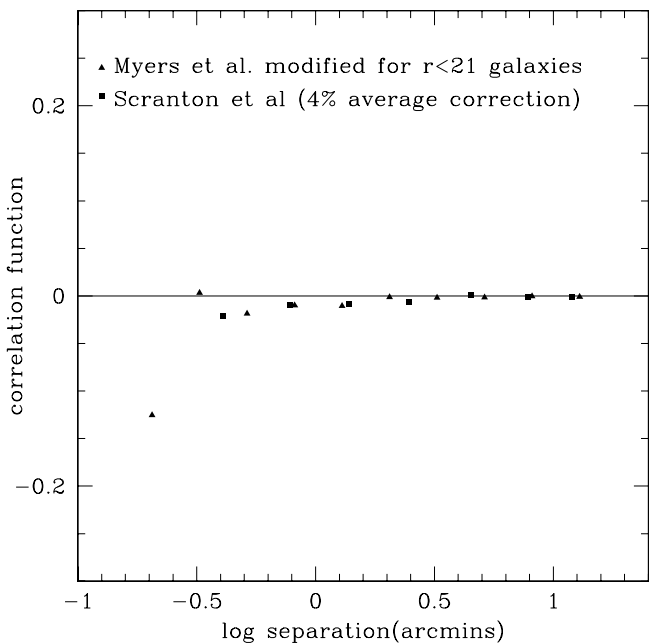


Figure 18. QSO-galaxy cross-correlations. The triangles show Myers et al. (2005) results modified for an $r < 21$ galaxy sample. Squares show the results from Scranton et al. averaged for 4% contamination as described in Section 5.7. The two results are in very good agreement.

to the SDSS galaxy correlation function. Previous authors (e.g. Colin et al. 1999) have suggested that in such models there can be anti-bias at the level of up to $b \approx 0.6$ on scales $0.1 < r < 1h^{-1}\text{Mpc}$ with $b \approx 1$ on larger scales. As discussed by Myers et al. (2005) significantly stronger anti-bias than this at $0.1 < r < 1h^{-1}\text{Mpc}$ was required by their galaxy-QSO lensing results (see their Fig. 10) and these results are now strengthened by the agreement found in the new SDSS QSO datasets of Scranton et al. as well as those analysed here. We believe that the factor of ≈ 6 that we are seeking is too large to be explained by some subtlety in the HOD prescription. We also note that Guimaraes, Myers & Shanks (2006) used the Hubble Volume simulation of the standard model to test if some subtlety in either galaxy or group assignment could explain the large anti-correlation as an artefact. However, these authors confirmed that approximately unbiased galaxy distributions assuming the standard cosmology were a factor of ≈ 10 away from explaining the amplitude of anti-correlation seen with either galaxies or galaxy groups and clusters.

We take our best data for the spectroscopic 2QZ sample which is the Northern 2QZ strip reported here, combined with the Southern 2QZ strip as reported by Myers et al. (2003) for galaxies, inversely weighted by variance. We find that a fit of $w_{qg}(\theta) = -0.023 \pm 0.006\theta^{-0.96 \pm 0.3}$ describes our data, where θ is expressed in arcminutes. The results are shown in Fig. 19. Open circles show the weighted average results for both strips and the short-dashed line shows our model. The new $N + S$ result is almost exactly the same as that of Myers et al. (see their eq. 21) and so our fitted galaxy bias remains $b_{0.1} = 0.13 \pm 0.06$ from the model of Williams & Irwin (1998). The same model gives $b_{0.1} = 0.32 \pm 0.15$ in the Einstein-de Sitter case. Here and below, the model of Gaztanaga (2003) would give proportionately smaller bias values (see Table 1 of Myers et al 2005).

We then take our best photometric DR1 5 areas QSO-galaxy result corrected for contamination as in Fig. 12. We find that a fit of $w_{qg}(\theta) = -0.007 \pm 0.005\theta^{-1.4 \pm 0.43}$ describes our data. In Fig. 19 filled circles show our results and the line shows our model. Scaling again via equation (19) of Myers et al. we find $b_{0.1} = 0.18 \pm 0.08$ for the standard cosmology in the Williams and Irwin case, in reasonable agreement with the result of Myers et al. In the Einstein-de Sitter case, the result gives $b_{0.1} = 0.44 \pm 0.20$.

Finally, we take the corrected Scranton et al. QSO-galaxy cross-correlation results (4% average correction) and find that a fit (Fig. 19) of $w_{qg}(\theta) = -0.009 \pm 0.003\theta^{-1.0 \pm 0.38}$. The squares in Fig. 19 show Scranton et al. results with a 4% average correction and the long dashed line shows our model. Scaling here via equation (19) of Myers et al. (2005) and taking into account their $r < 21$ galaxy limit gives $b_{0.1} = 0.14 \pm 0.06$ for the standard cosmology and $b_{0.1} = 0.32 \pm 0.15$ for the Einstein-de Sitter case under the assumptions of Williams & Irwin. Again these results are in reasonable agreement with those of Myers et al.

8 CLUSTER MODEL FITTING

Here we fit our best new data in terms of the cluster/group lensing effect. We, first, follow the modelling procedures of Myers et al. (2003) who assumed the mass distribution in

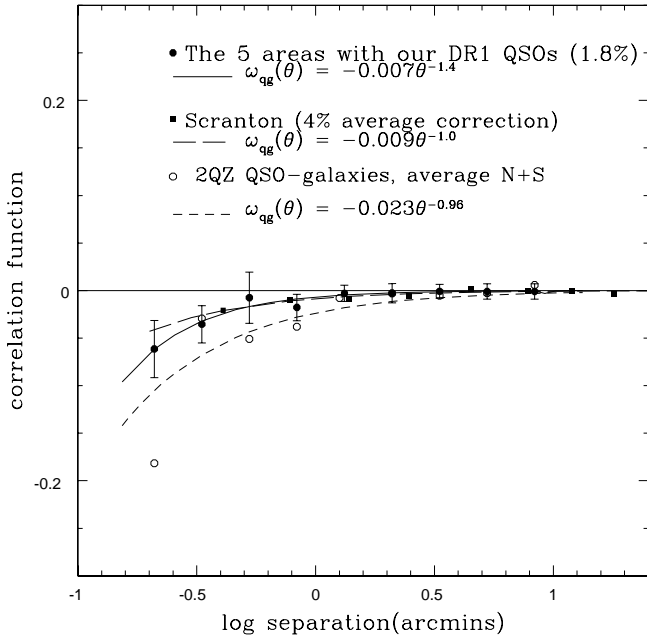


Figure 19. Our fits for our DR1 QSOs in the 5 areas (corrected for 1.8% contamination) and for Scranton et al. (4% average correction based on the $r < 21$ galaxy autocorrelation). The weighted averaged results from the NGC and SGC (Myers et al.) are shown by the open circles. The short dashed line shows our fit.

the groups followed a Singular Isothermal Sphere (SIS). Here sources are magnified by a factor

$$\mu = \frac{\theta}{\theta - 4\pi \frac{D_{ls}}{D_s} \left(\frac{\sigma}{c}\right)^2} \quad (3)$$

where D_{ls} is the distance between the lens and the source, D_s is the distance between the observer and the source, c is the speed of light, σ is the velocity dispersion of the SIS and θ is the angle between the source, the observer and the centre of the lens. The factor $4\pi \frac{D_{ls}}{D_s} \left(\frac{\sigma}{c}\right)^2$ is the Einstein radius, so $\theta_E = 4\pi \frac{D_{ls}}{D_s} \left(\frac{\sigma}{c}\right)^2$. Then the correlation function is given by $w(\theta) = \mu^{2.5\beta-1} - 1$, where β is the slope of the number-magnitude relation. When $\beta = 0.4$ then $w(\theta) = 0$, for higher values of β we observe a correlation and for lower values an anti-correlation (Myers et al.). Using the last two equations we can predict the form of the correlation function.

We also follow Myers et al. (2003) modelling procedures for determining the form of the correlation function based on lensing from dark matter haloes (NFW, Navarro, Frenk & White 1995). We use the NFW profile which describes haloes that have mass of 9 orders of magnitude, e.g. galaxy clusters. The form of this NFW profile is given (equation A7 in Myers et al. 2003)

$$\rho(r) = \frac{\delta_c \rho_c}{\frac{r}{r_s} \left(1 + \frac{r}{r_s}\right)^2} \quad (4)$$

where ρ_s is the critical density and r_s is a representative radial scale. Then, using equations (A2), (A8), (A9), (A10) and (A20) from Myers et al. (2003) we derive the magnifi-

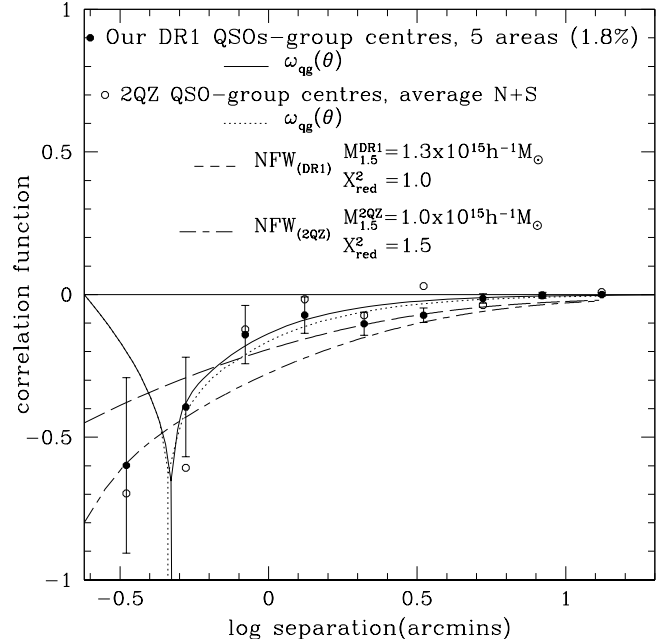


Figure 20. Our weighted average results for both the North and South strips are shown by the filled circles and the fit to them by the dotted line. The χ^2 fit for the cross-correlation of our DR1 QSOs and centres of groups in the 5 areas (corrected for 1.8% contamination) is shown by the solid line. 2QZ results are similarly represented by the open circles and the dotted line. The long dashed line shows the best fitting NFW model profile for the DR1 QSO-group centers cross-correlation and the long-short dashed line for the 2QZ QSO-group centers cross-correlation.

cation due to the lensing effect that comes from these dark matter haloes.

We take our best photometric DR1 5 areas dataset corrected for contamination as in Fig. 14 for centres of groups. Using a χ^2 fit after the fashion of Myers et al., we find that a velocity dispersion of 1040 km s^{-1} fits the $m > 7$ group data ($\chi_{red}^2 = 0.7$) and the SIS model is shown in Fig. 20 by the solid line. This is close to the value of 1156 km s^{-1} found by Myers et al. We, also fit the NFW profile which is shown by the long dashed line. The best NFW fit has a mass of $M_{1.5}^{DR1} = 1.3 \times 10^{15} h^{-1} M_\odot$ with $\chi_{red}^2 = 1.0$.

Finally, in a similar way as we did in the previous Section we combine our results from the cross-correlation of 2QZ QSOs with centres of groups in the NGC with Myers et al. results in the SGC and then we fit a model to our weighted average results (open circles, Fig. 20). Here our χ^2 fit for the SIS velocity dispersion yields 1060 km s^{-1} ($\chi_{red}^2 = 1.3$) again close to the value found by Myers et al. The SIS model is shown by the dotted line in Fig. 20. The NFW profile in this case yields a mass of $M_{1.5}^{2QZ} = 1.0 \times 10^{15} h^{-1} M_\odot$ with $\chi_{red}^2 = 1.5$.

9 DISCUSSION + CONCLUSION

Using a photometric QSO sample which was extracted by the same method as that of Scranton et al. we have inves-

tigated the reasons that their results appear different from Myers et al. (2005), giving a lower anti-correlation signal.

We first cross-correlated our DR1 SDSS QSO sample with galaxies ($g < 21$) and found that our results are in reasonable agreement with Myers et al. (2005) at least on scales larger than $1'$. 2QZ QSOs and DR1 QSOs cross-correlated with the same $g < 21$ galaxy sample give consistent results on scales larger than $1'$. The results of Scranton et al. show a smaller anti-correlation signal as expected from the different galaxy sample ($r < 21$) that they use. In the case of cross-correlations between QSO-galaxies in clusters, the results repeat the same pattern in that we detected anti-correlation consistent with the results of Myers et al. (2003) but at considerably higher S/N than for galaxies.

Then we checked the low-redshift contamination in the $1 < z_p < 2.2$ photometric SDSS QSO samples. We compared our sample with spectroscopic samples taken from the 2QZ catalogue, COSMOS field (Prescott et al.) and Λ CDM spectra that we observed for four new 2dF fields. The results show $\approx 2\%$ contamination in our photometric sample for spectroscopic redshift $z < 0.3$ and $\approx 4\%$ for $z < 0.6$. We then corrected our DR1 results and Scranton et al. results assuming these percentages of contamination. Then comparing the autocorrelation results from $g < 21$ and $r < 21$ galaxies we modified Myers et al. (2005) QSO-galaxy cross-correlation results and we found that the observational results are actually in very good agreement.

Therefore we have found that there are two reasons that Scranton et al. and Myers et al. results look different. The first is that the low-redshift contamination in the photometric QSO sample has not been taken into account and the second is that the galaxy sample used in each analysis is different. *When we account for these effects, we consider that the Scranton et al. SDSS results at faint magnitudes provide strong observational confirmation of the results of Myers et al. (2005, 2003) in the same QSO magnitude range.*

Correcting for low-redshift contamination also lowers the positive correlation claimed by Scranton et al. at bright magnitudes. However, in the $17 < g < 19.5$ bin of Scranton et al. some positive signal is still seen even after contamination correction, at an appropriate amplitude to match the anti-correlation seen at fainter magnitudes. But the strong anti-correlation seen at QSO limit $g < 21$ suggests that the relevant slope for $g < 19$ QSO samples ($\beta = 0.564$) is close to the critical $\beta = 0.4$ slope found at $19 < g < 20$. This means that little positive correlation is expected in this magnitude range despite the strong anti-correlation seen at fainter QSO magnitudes. We note that for cluster/group lensing the relevant slope may be in the $n(m)$ bin fainter than the QSO limit because this is where the QSOs sit before magnification.

This then leaves the question of why Myers et al. require a strong anti-bias of $b \approx 0.1$ in the standard cosmology to explain the faint QSO anti-correlation whereas Scranton et al. require $b \approx 1$. We have noted that Scranton et al. use a more complicated analysis than that of Myers et al. (2005), using the HOD of Zehavi et al. (2005). However, the HOD that they use appears to have $b \approx 0.6 - 1$ in the region of interest and it appears difficult to explain away the factor of 6 - 10 discrepancy by other subtleties in the HOD approach. Moreover, Guimaraes, Myers and Shanks (2005) used mock galaxy catalogues with $b \approx 1$ derived from the Hubble Volume simulation using standard parameters and

confirmed that models with $b \approx 1$ are a factor of ≈ 10 away from explaining the QSO magnification data.

With the SDSS results now observationally confirming the 2QZ results, we believe that QSO lensing has now come of age. We note there remain discrepancies with the $b \approx 1$ results found from weak-lensing cosmic shear results. However as noted by Hirata & Seljak (2004) there are serious potential problems with weak lensing shear results in that the effects of intrinsic galaxy alignments are difficult, if not impossible, to eliminate from the shear analysis. It is important to reconcile the QSO magnification and weak shear results for if it proves that our QSO magnification results are more accurate then the consequences for cosmology would be significant. For example, Shanks (2006) has noted the potential impact of the QSO magnification results on the interpretation of the acoustic peaks in the CMB.

10 ACKNOWLEDGMENTS

We thank A. D. Myers and A.C.C. Guimaraes for useful discussions.

Funding for the SDSS and SDSS-II has been provided by the Alfred P. Sloan Foundation, the Participating Institutions, the National Science Foundation, the U.S. Department of Energy, the National Aeronautics and Space Administration, the Japanese Monbukagakusho, the Max Planck Society, and the Higher Education Funding Council for England. The SDSS Web Site is <http://www.sdss.org>.

The SDSS is managed by the Astrophysical Research Consortium for the Participating Institutions. The Participating Institutions are the American Museum of Natural History, Astrophysical Institute Potsdam, University of Basel, Cambridge University, Case Western Reserve University, University of Chicago, Drexel University, Fermilab, the Institute for Advanced Study, the Japan Participation Group, John Hopkins University, the Joint Institute for Nuclear Astrophysics, the Kavli Institute for Particle Astrophysics and Cosmology, the Korean Scientist Group, the Chinese Academy of Sciences (LAMOST), Los Alamos National Observatory, the Max-Planck-Institute for Astronomy (MPIA), the Max-Planck-Institute for Astrophysics (MPA), New Mexico State University, Ohio State University, University of Pittsburgh, University of Portsmouth, Princeton University, the United States Naval Observatory, and the University of Washington.

The 2dF QSO Redshift Survey (2QZ) was compiled by the 2QZ survey team from observations made with the 2-degree Field on the Anglo-Australian Telescope.

References

- Bartelmann M., 1996, *A & A*, 313, 697
- Boyle B. J., Shanks T., Peterson B. A., 1988, *MNRAS*, 235, 935
- Broadhurst T., Lehar J., 1995, *ApJ*, 450, L41
- Colin P., Klypin, A.A., Kravstov, A.V. & Khokhlov, A.M. 1999, *ApJ*, 523, 32

- Croom S. M., Shanks T., 1996, MNRAS, 281, 893
- Croom S. M., Shanks T., 1999, MNRAS, 307, L17
- Croom S. M., Smith R. J., Boyle B. J., Shanks T., Miller L., Outram P.J., Loaring N. S., 2004 MNRAS, 349, 1397
- Gaztanaga E, 2003, ApJ, 589, 82
- Guimaraes A.C.C., Myers A.D., Shanks T., 2005, MNRAS, 362, 657
- Hirata C. M., Seljak U., 2004, Phys. Rev. D, 70, 063526
- Jain, B., Scranton, R. & Sheth, R.K., 2003 MNRAS, 345, 62
- Maoz D., Rix H. W., Gal-Yam A., Gould A., 1997, AJ, 486, 75
- Mellier, Y., Meylan G., 2005, Gravitational Lensing Impact on Cosmology (S225), Edited by Yannick Mellier and Georges Meylan, pp. . ISBN 0521851963. Cambridge, UK: Cambridge University Press, 2005
- Myers A. D., Outram P. J., Shanks T., Boyle B. J., Croom S. M., Loaring N. S., Miller L., Smith R. J., 2003, MNRAS, 342, 467
- Myers A.D., Shanks T., Boyle B.J., Croom S.M., Loaring N.S., Miller L. & Smith R.J. 2005, MNRAS, 359, 741.
- Myers A. D., 2003, PhD Thesis, University of Durham
- Myers, A.D. et al., 2007, astro-ph/0612190
- Navarro J. F., Frenk C. S., White S. D. M., 1995, ApJ, 275, 720
- Nollenberg, J. G., Williams L. L. R., 2005, ApJ, 634, 793
- Peebles P. J. E., 1980, The large scale structure in the Universe, Princeton Univeristy Press, ISBN 0-691-08240-5
- Prescott M. K. M., Impey C. D., Cool R. J., Scoville N.Z., Quasars in the COSMOS field, 2006, ApJ, 644, 100
- Richards G. T. et al., 2004, ApJS, 155, 257
- Scranton et al., 2005, ApJ, 633, 589
- Shanks T., 2006, MNRAS submitted, astro-ph/0609339
- Shanks T., Boyle B. J., 1994, MNRAS, 271, 753
- Sharp R.G. et al. 2006, MNRAS submitted, astro-ph/0606137
- Stevenson P. R. F., Fong R., Shanks T., 1988, MNRAS, 234, 801
- Weinstein M. A. et al., 2004, ApJS, 155, 243
- Williams L. L. R., Irwin M., 1998, MNRAS, 298, 378
- Wu X.P., 1994, A&A, 286, 748-752
- Zehavi, I. et al., 2005, ApJ, 630, 1